2956 *Langmuir* **2006,** *22,* 2956−2960

Preparation and Encapsulation of Highly Fluorescent Conjugated Polymer Nanoparticles

Changfeng Wu, Craig Szymanski, and Jason McNeill*

Department of Chemistry, Center for Optical Materials Science and Engineering Technologies, Clemson University, Clemson, South Carolina 29634

Received January 19, 2006

A facile method has been developed to prepare aqueous dispersions of encapsulated conjugated polymer nanoparticles exhibiting high fluorescence brightness. Salient features of the nanoparticles include their small diameter and spherical morphology. Encapsulation of the nanoparticles with a silica shell reduces the rate of photooxidation and allows facile attachment of functional groups for subsequent bioconjugation and nanoparticle assembly. Functionalization of the nanoparticle with amine groups followed by the addition of Au nanoparticles resulted in the formation of nanoparticle assemblies, as evidenced by the efficient quenching of the conjugated polymer fluorescence by the Au nanoparticles.

Introduction

Highly fluorescent nanoparticles have been demonstrated in a wide range of applications such as high-throughput screening, ultrasensitive assays, live cell imaging, and intracellular dynamics.[1−5] Currently available fluorescent nanoparticles include colloidal inorganic semiconductor quantum dots,[1−9] dye-loaded latex spheres,[10,11] and dye-doped silica colloids.[12−16] These nanoparticles possess high brightness and improved photostability as compared to conventional fluorescent dyes. However, cytotoxicity is a critical problem in any live-cell or animal experiments for the Cd-containing quantum dots.[17,18] There are also a number of limitations with the dye-loaded beads, such as the relatively large size (>30 nm) and limited dye-loading concentration due to self-quenching. A largely unexplored alternative is the use of encapsulated π-conjugated polymer particles as fluorescent labels. Many π-conjugated polymers are known to possess high extinction coefficients (typically 10^6−10^7 M^{-1}cm^{-1}) and high fluorescence quantum yields (∼80%).[19] Ultrasensitive detection schemes based on the efficient quenching of π-conjugated polyelectrolyte fluorescence in aqueous solution have been reported.[20−22]

There is growing interest in the preparation and optoelectronic applications of conjugated polymer nanoparticles.[23−25] A miniemulsion method was recently developed to prepare submicron-sized conjugated polymer particles (∼0.1 μm diameter),[23−25] and device layers with controlled domain sizes were achieved by casting from mixtures of suspended particles.[25] Another approach based on reprecipitation has also been applied to obtain polythiophene nanoparticles.[26] These approaches prepare particles with a diameter of ∼30 nm or higher that consist of hundreds of polymer molecules. Here, we demonstrate an alternate method for obtaining hydrophobic conjugated polymer nanoparticles dispersed in water. In terms of suitability for fluorescence labeling applications, the features of the particles produced by this method, including their small size (∼10 nm), high extinction coefficients (as high as 5×10^7 M^{-1} cm^{-1}), and adequate quantum yield (10%), compare favorably to quantum dots.[19,27,28] Further growth of thin silica shells on the polymer nanoparticles provides the additional benefit of facilitating biofunctionalization and improving photostability. Efficient fluorescence quenching of the encapsulated polymer nanoparticles by metal nanoparticles is also observed, indicating the potential of this novel type of fluorescent nanoparticle for a variety of sensing applications.

Experimental Section

Materials. The conjugated polymers employed in this study are the polyfluorene derivative poly(9,9-dihexylfluorenyl-2,7-diyl) (PFO; average MW = 55 000; polydispersity = 2.7), the copolymer poly-

---

* Corresponding author. E-mail: mcneill@clemson.edu.

(1) Jaiswal, J. K.; Mattoussi, H.; Mauro, J. M.; Simon, S. M. *Nat. Biotechnol.* **2003**, *21*, 47−51.

(2) Alivisatos, P. *Nat. Biotechnol.* **2004**, *22*, 47−52.

(3) Medintz, I. L.; Uyeda, H. T.; Goldman, E. R.; Mattoussi, H. *Nat. Mater.* **2005**, *4*, 435−446.

(4) Alivisatos, A. P.; Gu, W. W.; Larabell, C. *Annu. Rev. Biomed. Eng.* **2005**, *7*, 55−76.

(5) Michalet, X.; Pinaud, F. F.; Bentolila, L. A.; Tsay, J. M.; Doose, S.; Li, J. J.; Sundaresan, G.; Wu, A. M.; Gambhir, S. S.; Weiss, S. *Science* **2005**, *307*, 538−544.

(6) Bruchez, M.; Moronne, M.; Gin, P.; Weiss, S.; Alivisatos, A. P. *Science* **1998**, *281*, 2013−2016.

(7) Chan, W. C. W.; Nie, S. M. *Science* **1998**, *281*, 2016−2018.

(8) Gao, X.; Cui, Y.; Levenson, R. M.; Chung, L. W. K.; Nie, S. *Nat. Biotechnol.* **2004**, *22*, 969−976.

(9) Wu, X. Y.; Liu, H. J.; Liu, J. Q.; Haley, K. N.; Treadway, J. A.; Larson, J. P.; Ge, N. F.; Peale, F.; Bruchez, M. P. *Nat. Biotechnol.* **2003**, *21*, 41−46.

(10) Yang, C. S.; Chang, C. H.; Tsai, P. J.; Chen, W. Y.; Tseng, F. G.; Lo, L. W. *Anal. Chem.* **2004**, *76*, 4465−4471.

(11) Kolodny, L. A.; Willard, D. M.; Carillo, L. L.; Nelson, M. W.; Van Orden, A. *Anal. Chem.* **2001**, *73*, 1959−1966.

(12) Santra, S.; Wang, K.; Tapec, R.; Tan, W. *Anal. Chem.* **2001**, *73*, 4988−4993.

(13) Zhao, X. J.; Hilliard, L. R.; Mechery, S. J.; Wang, Y. P.; Bagwe, R. P.; Jin, S. G.; Tan, W. H. *Proc. Natl. Acad. Sci. U.S.A.* **2004**, *101*, 15027−15032.

(14) Ow, H.; Larson, D. R.; Srivastava, M.; Baird, B. A.; Webb, W. W.; Wiesner, U. *Nano Lett.* **2005**, *5*, 113−117.

(15) Wang, L.; Yang, C. Y.; Tan, W. H. *Nano Lett.* **2005**, *5*, 37−43.

(16) Graf, C.; Schartl, W.; Fischer, K.; Hugenberg, N.; Schmidt, M. *Langmuir* **1999**, *15*, 6170−6180.

(17) Derfus, A. M.; Chan, W. C. W.; Bhatia, S. N. *Nano Lett.* **2004**, *4*, 11−18.

(18) Kirchner, C.; Liedl, T.; Kudera, S.; Pellegrino, T.; Javier, A. M.; Gaub, H. E.; Stolzle, S.; Fertig, N.; Parak, W. J. *Nano Lett.* **2005**, *5*, 331−338.

(19) Pei, Q. B.; Yang, Y. *J. Am. Chem. Soc.* **1996**, *118*, 7416−7417.

(20) Chen, L.; McBranch, D. W.; Wang, H. L.; Helgeson, R.; Wudl, F.; Whitten, D. G. *Proc. Nat. Acad. Sci. U.S.A.* **1999**, *96*, 12287−12292.

(21) Heeger, P. S.; Heeger, A. J. *Proc. Natl. Acad. Sci. U.S.A.* **1999**, *96*, 12219−12221.

(22) Fan, C. H.; Wang, S.; Hong, J. W.; Bazan, G. C.; Plaxco, K. W.; Heeger, A. J. *Proc. Natl. Acad. Sci. U.S.A.* **2003**, *100*, 6297−6301.

(23) Landfester, K. *Adv. Mater.* **2001**, *13*, 765−768.

(24) Landfester, K.; Montenegro, R.; Scherf, U.; Guntner, R.; Asawapirom, U.; Patil, S.; Neher, D.; Kietzke, T. *Adv. Mater.* **2002**, *14*, 651−655.

(25) Kietzke, T.; Neher, D.; Landfester, K.; Montenegro, R.; Guntner, R.; Scherf, U. *Nat. Mater.* **2003**, *2*, 408−412.

(26) Kurokawa, N.; Yoshikawa, H.; Hirota, N.; Hyodo, K.; Masuhara, H. *ChemPhysChem* **2004**, *5*, 1609−1615.

(27) Leatherdale, C. A.; Woo, W. K.; Mikulec, F. V.; Bawendi, M. G. *J. Phys. Chem. B* **2002**, *106*, 7619−7622.

(28) Tsay, J. M.; Doose, S.; Pinaud, F.; Weiss, S. *J. Phys. Chem. B* **2005**, *109*, 1669−1674.

10.1021/la060188l CCC: $33.50

[{9,9-dioctyl-2,7-divinylene-fluorenylene}-*alt*-co-{2-methoxy-5-(2-ethylhexyloxy)-1,4-phenylene}] (PFPV, average MW = 270 000, polydispersity = 2.7), and the polyphenylenevinylene derivative poly[2-methoxy-5-(2-ethylhexyloxy)-1,4-phenylenevinylene] (MEH−PPV, average MW = 200 000, polydispersity = 7.0). All polymers were purchased from American Dye Source (Quebec, Canada). Tetrahydrofuran (THF, anhydrous, 99.9%), octyltrimethoxysilane (OTMOS, 96%), 3-aminopropyltrimethoxysilane (APTMS, 97%), sodium citrate, and sodium silicate solution (27% SiO_2) were purchased from Aldrich (Milwaukee, WI). Hydrogen tetrachloroaurate (99.9%) was purchased from Alfa Aesar (Ward Hill, MA). All chemicals were used without further purification.

Nanoparticle Preparation. Conjugated polymer was dissolved by stirring overnight in THF under inert atmosphere. The solution was then filtered through a 1.6 μm filter and further diluted to a concentration of 20 ppm. A 2 mL quantity of the polymer/THF solution was added quickly to 8 mL of deionized water while sonicating the mixture. The suspension was filtered with a 0.2 μm membrane filter. The THF was removed by partial evaporation under vacuum, followed by filtration through a 0.2 μm filter. The overall yield of the nanoparticles was typically higher than 80%. The resulting nanoparticle dispersions were clear, with colors similar to those of the polymers in THF solution.

Silica Encapsulation. The silica encapsulation is achieved by a two-step method. At the first step of nanoparticle preparation, 0.05 g of OTMOS in ethanol solution (0.08%) was added to 10 mL of a 5 ppm nanoparticle dispersion before the evaporation of THF, then rocked for 30 min. THF was then removed by partial vacuum evaporation. Further growth of a silica shell is based on the polymerization of active silica. A solution of active silica was prepared by lowering the pH of a 0.54% sodium silicate solution to 10−11 by the progressive addition of cation-exchange resin (Amberlite IR120, 16−50 mesh).[29,30] A 0.5 mL portion of active silica was added to a 10 mL suspension of silane-modified polymer nanoparticles. The mixture was allowed to stand for 24 h under vigorous stirring so that the active silica polymerized onto the nanoparticle surface. The silica shell thickness was about 2−4 nm after 24 h. The dispersion was then dialyzed against deionized water for 48 h to remove excess silica.

Formation of Gold Nanoparticle Assemblies. Gold nanoparticles were prepared according to the standard sodium citrate reduction method.[31] A 1.0 mL portion of the sodium citrate solution (34 mM) was added to 50 mL of boiled chlorauric acid solution (0.25 mM) while stirring. The obtained gold nanoparticles had an average diameter of 15 nm with 10% size dispersity. A silane coupling agent (APTMS) was used to assemble the silica-coated polymer nanoparticles with gold nanoparticles. A 20 μL portion of the APTMS solution (0.2 wt %) was added to a suspension of silica-encapsulated PFPV nanoparticles (5 mL, 16 nM) and rocked for 1 h. The amount of APTMS was calculated to coat the nanoparticles with one monolayer. A 5 mL portion of the amine-functionalized PFPV nanoparticles (16 nM) was then mixed with 5 mL of gold nanoparticles (1 nM). The mixture was allowed to stand for 2 h prior to spectroscopic measurements. A similar procedure was used to assemble MEH−PPV with gold nanoparticles, and the resulting dispersion contained MEH−PPV and gold with 12 nM and 0.5 nM concentrations, respectively.

Characterization Methods. The size, shape, and size distribution of the polymer nanoparticles were characterized by atomic force microscopy (AFM). For these measurements, one drop of the nanoparticle dispersion was placed on freshly cleaned silicon substrate. After evaporation of the water, the surface was scanned with a Digital Instruments multimode AFM in tapping mode. The nanoparticle and polymer−gold nanoparticle assemblies were also characterized by transmission electron microscopy (TEM). Small drops of the nanoparticle dispersion were placed on copper grids coated with carbon film, and dried in air. TEM images were taken on a Hitachi H-7600 microscope with 120 kV accelerating voltage. The UV−vis absorption spectra were recorded with a Shimadzu UV-2101PC UV−vis scanning spectrophotometer using quartz cuvettes with an optical path of 1 cm. Fluorescence spectra were collected with a PTI fluorometer (Photon Technology International) using a 1 cm quartz cuvette.

Results and Discussion

We recently developed a facile procedure for preparing an aqueous dispersion of nanoparticles consisting of single molecules of the conjugated polymer MEH−PPV.[32] Here, we prepare small nanoparticles (∼10 nm) of a variety of hydrophobic conjugated polymers. To our knowledge, there are no reports in the literature for preparing aqueous dispersions of hydrophobic conjugated polymer nanoparticles in this size range. Our preparation method is modified from the reprecipitation procedure employed by Kurokawa and co-workers,[26] which involves rapid addition of a polymer solution (prepared with a water-miscible organic solvent) to water. By employing a very dilute solution (<20 ppm) and brief sonication to improve mixing, particles were obtained with much smaller diameters (∼10 nm versus 30 nm) as compared to previous reports using the reprecipitation and the miniemulsion methods.[23−26]

Nanoparticle dispersions of conjugated polymers PFO, PFPV, and MEH−PPV were prepared. The dispersions are clear (not turbid), with colors similar to those of the polymers in THF solution. The nanoparticles are stable for weeks, with no evidence of aggregation or decomposition. The dispersions were drop-cast onto silicon substrates for analysis of nanoparticle size and morphology by tapping-mode AFM. Figure 1 shows the AFM images of various nanoparticles on silicon substrates. The nanoparticles exhibit a roughly spherical morphology, and they can form either a densely packed layer (Figure 1a) or a sparse layer of well-separated nanoparticles (Figure 1b,c), depending on the drop-casting conditions. Detailed analysis of the particle morphology indicates that the majority of particles are approximately spherical in shape. Further indication that most particles are approximately spherical is that the aspect ratio obtained from the AFM images of the nanoparticles is similar to that obtained for 20 nm latex spheres (Molecular Probes). In addition, the nearest-neighbor spacing of dense arrays is similar (within measurement uncertainty) to the particle height. The observation of approximately spherical morphology is somewhat surprising, considering that the rigid backbone of conjugated polymers is known to exert a large influence over polymer conformation.[33,34] However, given the large interfacial surface tension between the polymer and water, a collapsed, roughly spherical polymer conformation is thermodynamically favored, even for somewhat rigid polymers.[35,36] Additionally, there is evidence that the vinylene linkages are not as rigid as previously believed; some calculations have indicated that the energy required to bend a conjugated polymer chain by generating a tetrahedral defect is thermally accessible.[37]

A particle height analysis was done on AFM images of sparse layers, and the corresponding histograms are shown in Figure 1 (right). The majority of nanoparticle diameters are in the range

---

[29] Alejandro-Arellano, M.; Ung, T.; Blanco, A.; Mulvaney, P.; Liz-Marzan, L. M. *Pure Appl. Chem.* **2000**, *72*, 257−267.

[30] Liz-Marzan, L. M.; Giersig, M.; Mulvaney, P. *Langmuir* **1996**, *12*, 4329−4335.

[31] Enüstün, B. V.; Turkevich, J. *J. Am. Chem. Soc.* **1963**, *85*, 3317−3328.

[32] Szymanski, C.; Wu, C.; Hooper, J.; Salazar, M. A.; Perdomo, A.; Dukes, A.; McNeill, J. D. *J. Phys. Chem. B* **2005**, *109*, 8543−8546.

[33] Schwartz, B. J. *Annu. Rev. Phys. Chem.* **2003**, *54*, 141−172.

[34] Hu, D.; Yu, J.; Wong, K.; Bagchi, B.; Rossky, P. J.; Barbara, P. F. *Nature* **2000**, *405*, 1030−1033.

[35] Chandler, D. *Nature* **2005**, *437*, 640−647.

[36] ten Wolde, P. R.; Chandler, D. *Proc. Natl. Acad. Sci. U.S.A.* **2002**, *99*, 6539−6543.

[37] Wong, K. F.; Skaf, M. S.; Yang, C.-Y.; Rossky, P. J.; Bagchi, B.; Hu, D.; Yu, J.; Barbara, P. F. *J. Phys. Chem. B* **2001**, *105*, 6103−6107.

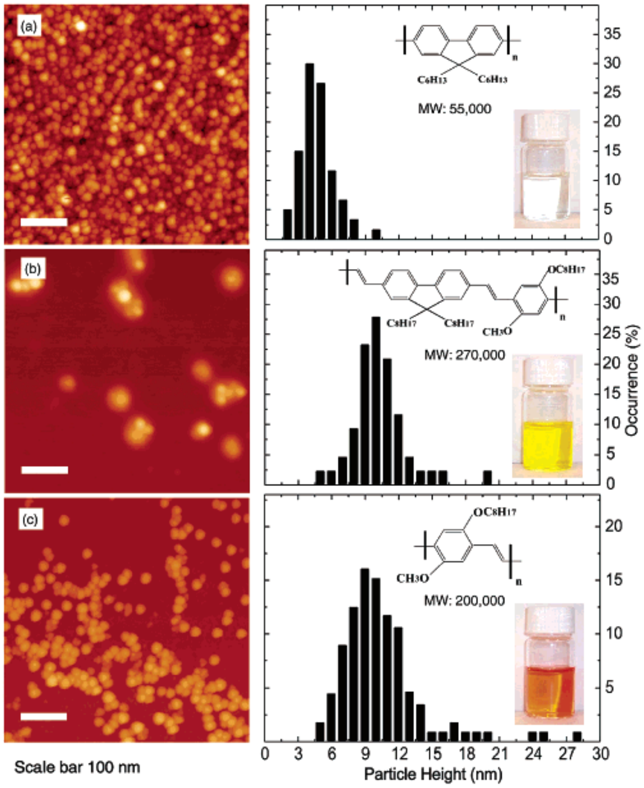

Figure 1. AFM images of the densely packed PFO nanoparticles (a), sparsely dispersed PFPV (b), and MEH−PPV nanoparticles (c) on silicon substrates. The corresponding histograms of the nanoparticle height are presented in the right side. The inset shows the molecular structures, molecular weight of the starting conjugated polymers, and the photographs of the resulting nanoparticle aqueous dispersions.

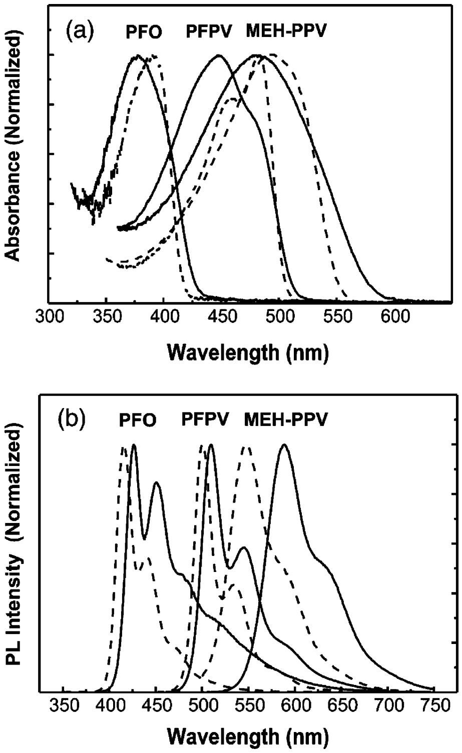

Figure 2. Normalized absorption (a) and fluorescence spectra (b) of the conjugated polymer nanoparticle dispersions (solid lines) as compared to the polymers in THF solutions (dashed lines).

of 3−7, 8−12, and 5−14 nm for PFO, PFPV, and MEH−PPV nanoparticles, respectively. The average diameters of the nanoparticles are consistent with roughly spherical single molecules of conjugated polymer, assuming tight packing of the polymer chain. For MEH−PPV, the much larger size range is attributable to the large polydispersity of the precursor polymer. It should be noted that the particle size depends on the starting concentration of polymer in THF. While there are batch-to-batch variations (with a small fraction of aggregates), the size distributions of the nanoparticles prepared from a starting solution of less than 20 ppm are consistent with roughly spherical single molecules of conjugated polymer with the molecular weight and polydispersity of the precursor polymer. Higher concentrations of the polymer solution resulted in the formation of larger particles. Here we limit our investigation to the smaller, primarily single-molecule nanoparticles. Although the size distributions of the polymer particles are relatively broad compared to those of quantum dots and dye-loaded beads, the size range should not present problems for many applications. Unlike quantum dots, the spectra of the polymer particles are relatively insensitive to particle size.[26] If necessary, improved control of the particle size could likely be achieved by reducing the polydispersity of the precursor polymer.

The particles dispersed in water exhibit broadened, blue-shifted absorption (Figure 2a, solid lines) and red-shifted fluorescence spectra (Figure 2b, solid lines) as compared to those of the polymer/THF solution (dashed lines). The observed blue-shift of the absorption peaks is consistent with an overall decrease in the conjugation length,[38] attributable to the bending or kinking of the polymer backbone. This is in agreement with simple geometric considerations: the diameter of a nanoparticle is roughly 50% of the effective conjugation length (∼12 repeat units) of the unconstrained polymer.[39] A red tail is also evident in the absorption spectra of polymer nanoparticles, indicating the presence of aggregate states due to interactions between segments of the polymer chain.[40] The absorption spectrum of the PFPV nanoparticles exhibits a change in the relative intensity of the two bands as compared to the spectrum of the polymer in solution. Similar effects are observed for many aggregates of π-conjugated molecules.[41] The fluorescence spectra of PFO, PFPV, and MEH−PPV nanoparticles are red-shifted by 15, 10, and 40 nm, respectively, as compared to those of the polymer in THF solutions. Since the nanoparticles possess a compact conformation, the red-shift in fluorescence could be ascribed to increased interactions between segments of the polymer chain, leading to energy transfer to low-energy chromophores and weakly fluorescent intrachain aggregates.[42,43] This is consistent with the reduction in quantum yield, where there is about a 4-fold decrease for PFO, a 7-fold decrease for PFPV and a 25-fold decrease for MEH−PPV nanoparticles, as compared to that of polymer in THF solutions. A fluorescence quantum yield of 10% and peak extinction coefficient of 5×10^7 $M^{-1}cm^{-1}$ was determined for PFPV nanoparticles suspended in water. A dilute solution of coumarin 6 in ethanol was used as a standard for quantum yield determination.[44] At a given low excitation intensity, the fluorescence intensity is proportional to the product of the extinction coefficient and the quantum yield. A comparison to the quantum yield and peak extinction coefficient of the

---

(38) Padmanaban, G.; Ramakrishnan, S. *J. Am. Chem. Soc.* **2000**, *122*, 2244−2251.

(39) Klaerner, G.; Miller, R. D. *Macromolecules* **1998**, *31*, 2007−2009.

(40) Nguyen, T. Q.; Doan, V.; Schwartz, B. J. *J. Chem. Phys.* **1999**, *110*, 4068−4078.

(41) Spano, F. C. *J. Chem. Phys.* **2005**, *122*, 234701.

(42) Padmanaban, G.; Ramakrishnan, S. *J. Phys. Chem. B* **2004**, *108*, 14933−14941.

(43) Martini, I. B.; Smith, A. D.; Schwartz, B. J. *Phys. Rev. B* **2004**, *69*, 35204.

(44) Reynolds, G. A.; Drexhage, K. H. *Opt. Commun.* **1975**, *13*, 222−225.

fluorescent dye rhodamine 6G indicates that the PFPV nanoparticles are more than 50 times brighter than rhodamine 6G. The fluorescence brightness of quantum dots has been reported to be in the range of 20 times that of rhodamine dyes.[7,45] Dye-loaded silica particles are reported to have a brightness equivalent to approximately 100 rhodamine molecules, but it should be noted that the silica particles are much larger (~30 nm in diameter) than the PFPV nanoparticles.[14] The high brightness of the nanoparticles is promising for biological labeling and sensing applications.

Encapsulation is a widely used strategy to facilitate the biofunctionalization of nanoparticles,[9,14] and can yield improvements in photostability and quantum yield.[6,7,46,47] Condensation of active silica or alkoxysilanes on a particle surface to form a silica shell is a proven method for particle encapsulation and also provides a surface that can be further functionalized by a variety of methods.[13,15,29,30,48,49] The presence of oxide or hydroxy groups on the surface of the nanoparticle is required to promote adhesion and polymerization of a silica shell. Therefore, a promoter is required for shell formation on noble metal or hydrophobic polymer particles.[30,50] Here, we chose OTMOS to promote silica shell formation. After the preparation of a nanoparticle dispersion, 0.05 g of an OTMOS/ethanol solution (0.08 wt %) was introduced to 10 mL of a 5 ppm nanoparticle solution, and the THF was removed by evaporation. Hydrolysis of the alkoxy groups resulted in the formation of a rigid micelle-like structure around the polymer core with oxygen bridges between the silicon atoms and silanol groups on the surface, as illustrated in Figure 3 (top).[51] The spectra of the encapsulated nanoparticles are identical to the spectra of the unencapsulated nanoparticles, indicating little effect on polymer conformation. A 2−3 nm thick silica shell is formed by the subsequent addition and polymerization of active silica.[29,30] Excess active silica was removed by dialysis. The encapsulated nanoparticles were characterized by TEM and energy-dispersive X-ray (EDX) spectrometry and were found to be spherical with diameters ranging from 10 to 18 nm, as shown in Figure 3b. EDX composition mapping images (not shown) indicate the presence of a silica shell and carbon in the core.

As an additional test of the silica encapsulation of the nanoparticles, the binding of surface-functionalized nanoparticles to gold nanoparticles was characterized by fluorescence spectroscopy and TEM. Gold nanoparticles have been found to efficiently quench the fluorescence of water-soluble conjugated polymers, as indicated by extremely large Stern−Volmer constants (K_{SV}).[22] The gold nanoparticles (15 nm) were prepared according to the standard sodium citrate reduction method.[31] The silica-encapsulated polymer nanoparticles were functionalized with amine groups using a silane coupling agent (APTMS). Amines are known to bind strongly to the surface of gold nanoparticles.[30,52] TEM observations (Figure 3c) indicate the coexistence of single gold/polymer nanostructures and some gold/polymer aggregates. It is clearly observed that each gold nanoparticle was coated with a rough shell composed of several silica-encapsulated polymer nanoparticles. Spectroscopic measurements were performed on the two aqueous dispersions of the Au/PFPV and Au/MEH−PPV nanostructures, one of which contains PFPV (8 nM) and gold nanoparticles (0.5 nM), the other has MEH−PPV (12 nM) and gold (0.5 nM). Binding with gold nanoparticles resulted in fluorescence quenching of ~33% for PFPV and ~50% for MEH−PPV nanoparticles. Assuming a linear Stern−Volmer relation in the experimental concentration range, the K_{SV} values were estimated to be quite large: $\sim 1 \times 10^9$ M^{-1} for PFPV and $\sim 2 \times 10^9$ M^{-1} for MEH−PPV, similar to the "hyperquenching" reported for conjugated polymer electrolytes complexed with Au nanoparticles.[22] Fluorescence spectra of free polymer and gold nanoparticle mixtures in the absence of APTMS indicated no quenching except for a small inner filter effect.[53] While the quenching mechanism has not yet been fully investigated, it is likely that the efficient quenching is due to the large extinction coefficient of the Au nanoparticle,[22,54] with perhaps some contribution being due to fast intraparticle energy transfer within the conjugated polymer nanoparticle.[32,55] Electron transfer has also been observed as a mechanism for quenching conjugated polymer fluorescence,[20] but, in this case, electron transfer is likely blocked by the silica shell.

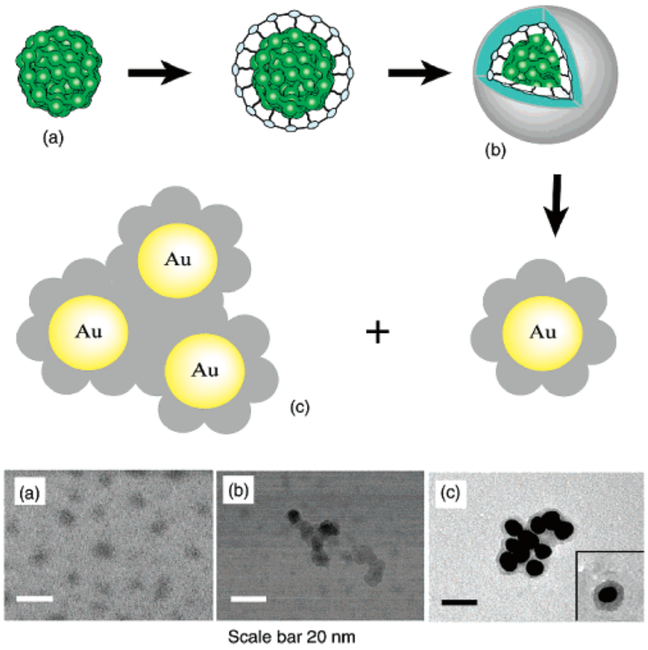

Figure 3. Schematic representation (top) of silica encapsulation of the conjugated polymer nanoparticles and assemblies of polymer/Au nanostructures. TEM images (bottom) of bare MEH−PPV nanoparticles (a), a silica-encapsulated nanoparticle (b), and assembled MEH−PPV/Au nanostructures (c).

Conclusions

In summary, we have demonstrated a method for preparing single conjugated polymer molecule nanoparticles encapsulated with silica. The nanoparticles are characterized by their high fluorescence brightness and small diameters. Amine-functionalized nanoparticles were also prepared. The nanoparticle fluorescence is efficiently quenched by Au nanoparticles via resonance energy transfer. The conjugated polymer nanoparticles are promising for fluorescence labeling and sensing applications

---

(45) Hohng, S.; Ha, T. *ChemPhysChem* **2005**, *6*, 956−960.

(46) Zhao, D.; Qin, W. P.; Wu, C. F.; Qin, G. S.; Zhang, J. S.; Lu, S. Z. *Chem. Phys. Lett.* **2004**, *388*, 400−405.

(47) Zhao, D.; Qin, W. P.; Zhang, J. S.; Wu, C. F.; Qin, G. S.; De, G. J. H.; Zhang, J. S.; Lu, S. Z. *Chem. Phys. Lett.* **2005**, *403*, 129−134.

(48) Chan, Y.; Zimmer, J. P.; Stroh, M.; Steckel, J. S.; Jain, R. K.; Bawendi, M. G. *Adv. Mater.* **2004**, *16*, 2092−2097.

(49) Zhao, X. J.; Tapec-Dytioco, R.; Tan, W. H. *J. Am. Chem. Soc.* **2003**, *125*, 11474−11475.

(50) Graf, C.; van Blaaderen, A. *Langmuir* **2002**, *18*, 524−534.

(51) Das, S.; Jain, T. K.; Maitra, A. *J. Colloid Interface Sci.* **2002**, *252*, 82−88.

(52) Oldenburg, S. J.; Averitt, R. D.; Westcott, S. L.; Halas, N. J. *Chem. Phys. Lett.* **1998**, *288*, 243−247.

(53) Lakowicz, J. R. *Principles of Fluorescence Spectroscopy*; Plenum Press: New York, 1999.

(54) Dubertret, B.; Calame, M.; Libchaber, A. J. *Nat. Biotechnol.* **2001**, *19*, 365−370.

(55) Yu, Z. H.; Barbara, P. F. *J. Phys. Chem. B* **2004**, *108*, 11321−11326.

because of the high brightness, small diameters, and efficient fluorescence quenching by metal nanoparticles.

Acknowledgment. The authors gratefully acknowledge financial support from Clemson University, NSF-EPSCoR, and an NSF-CAREER Award. We would also like to thank Dvora Perahia and Yunfei Jiang for their assistance in AFM measurements.

LA060188L